2024 IEEE/RSJ International Conference on Intelligent Robots and Systems (IROS)
October 14-18, 2024. Abu Dhabi, UAE

Reducing Cognitive Load in Teleoperating Swarms of Robots through a Data-Driven Shared Control Approach

Enrico Turco[1], Chiara Castellani[1], Valerio Bo[1],
Claudio Pacchierotti[2], Domenico Prattichizzo[1,3], and Tommaso Lisini Baldi[1,3]

***Abstract*— Multi-robot systems have gained increasing interest across various fields such as medicine, environmental monitoring, and more. Despite the evident advantages, the coordination of the swarm arises significant challenges for human operators, particularly concerning the cognitive burden needed for efficiently controlling the robots. In this study, we present a novel approach for enabling a human operator to effectively control the motion of multiple robots. Leveraging a shared control data-driven approach, we enable a single user to control the 9 degrees of freedom related to the pose and shape of a swarm. Our methodology was evaluated through an experimental campaign conducted in simulated 3D environments featuring a narrow cylindrical path, which could represent, e.g., blood vessels, industrial pipes. Subjective measures of cognitive load were assessed using a post-experiment questionnaire, comparing different levels of autonomy of the system. Results show substantial reductions in operator cognitive load when compared to conventional teleoperation techniques, accompanied by enhancements in task performance, including reduced completion times and fewer instances of contact with obstacles. This research underscores the efficacy of our approach in enhancing human-robot interaction and improving operational efficiency in multi-robot systems.**

I. Introduction

Multi-robot systems are emerging as an important area of research due to their potential to impact various fields, including search and rescue operations, environmental monitoring, medical robotics, and industrial automation. One example is the utilization of swarms of drones for tasks such as surveillance, disaster response, and agricultural monitoring. These systems leverage the collective intelligence and coordination of multiple robots to achieve tasks that would be impractical or impossible for a single robot to accomplish efficiently [1], [2]. Ground mobile robots represent another significant application of multi-robot systems, particularly in scenarios requiring exploration, mapping, or transportation tasks in challenging environments. These robots can collaborate to cover larger areas, share information, and effectively adapt to dynamic conditions. In the field of medical interventions, microrobots designed for endovascular procedures and surgeries [3] offer precise control and minimally invasive capabilities [4], [5]. Their small size enables access to intricate anatomical structures with reduced risk to patients. The effective utilization of such robots has already been demonstrated, with applications including targeted drug delivery [6], minimally-invasive surgical procedures [7], and diagnostics [8].

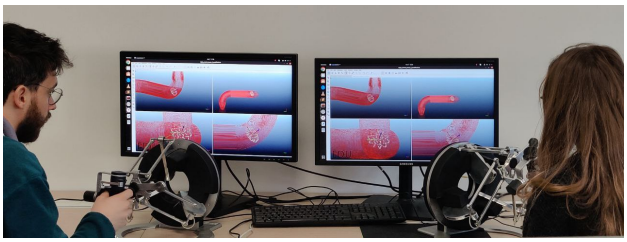

(a)

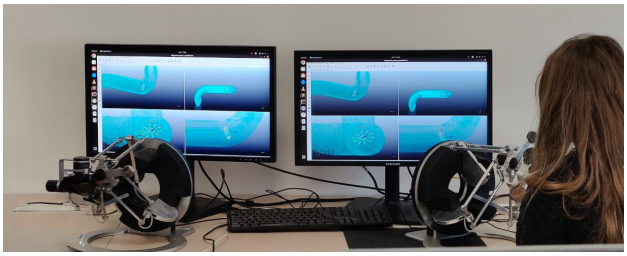

(b)

Fig. 1: In a), two operators collaboratively control the 9 DoFs of the robotic swarm using two interfaces. Conversely, b) illustrates the effectiveness of the proposed method, in which a single operator skillfully steers the swarm to complete a task, exploiting our novel shared control strategy. This method simplifies the control by assigning a subset of the degrees of freedom to the user, significantly reducing the operational complexity and enhancing user capability.

While the advantages of multi-robot systems are evident, the complexity of coordinating multiple independent agents poses challenges for human operators. Controlling the motion of numerous robots simultaneously in an intuitive and effective manner requires sophisticated interfaces and algorithms. Ensuring seamless interaction between humans and multi-robot systems is crucial for maximizing their potential benefits while minimizing operational complexities, safety risks, human-robot trust, and the cognitive load imposed on users during control [9]. An emphasis on user-centric design is essential for unlocking the potential of multi-robot systems

[1]Istituto Italiano di Tecnologia, Genoa, Italy {name.surname}@iit.it
[2]CNRS, Univ Rennes, Inria, IRISA – Rennes, France. {name.surname}@irisa.fr
[3]Università degli Studi di Siena, Dip. di Ingegneria dell'Informazione e Scienze Matematiche, Siena, Italy. {name.surname}@unisi.it

This work was supported by the European Union's Horizon Europe Research and Innovation Programme under Grant Agreement #101070066, project REGO, by the University of Siena curiosity driven (F-CUR) programme project "BRIOCHE: wearaBle sensoRImOtor interfaCes for Human augmentation", and by the European Union's FSE REACT-EU programme, PON Ricerca e Innovazione 2014-2020

across a wide range of applications. In this respect, different approaches have been developed to enable human users to effectively control multiple robots. Shared control techniques focus on distributing control responsibilities between humans and autonomous systems [10]. These methods aim to enhance human-robot collaboration by combining the decision-making capabilities of both entities, leading to improved task performance and operational efficiency. Similarly, shifting autonomy approaches emphasize the dynamic adjustment of robot autonomy levels based on the task requirements and environmental conditions [11]. By allowing robots to adapt their autonomy level in real time, these approaches enhance the flexibility and responsiveness of robotic systems. Furthermore, distributed approaches have been proposed to address the challenges associated with coordinating robots [12], [13]. Finally, research focusing on neural learning-based control for multi-robot systems aims to leverage advanced machine learning techniques to enhance coordination and decision-making processes among multiple robots [14], [15].

Research has shown that increasing robot autonomy can reduce the users' cognitive load [16]. This is due to the fact that the cognitive load depends on the number of conceptual elements users need to hold in mind simultaneously to accomplish a specific task [17]. However, while the autonomy level influences the teleoperator's perceived cognitive load and trust, there is no clear interaction between these latter factors [9]. In this context, we can consider each degree of freedom (DoF) of our robotic system as a conceptual element; therefore, minimizing the number of DoFs the users need to control is expected to reduce their cognitive load.

This paper presents a data-driven shared-control approach designed to dynamically allocate the controlled DoFs of a multi-robot system between the human operator and an autonomous controller, seeking the best compromise between the effectiveness of the control and the demanded cognitive load. We leverage statistical analysis on data collected from human demonstrations to design the shared control strategies, which are then evaluated in a human-subjects experiment where users control a simulated swarm in a narrow and tortuous environment. Through such collaborative control mechanisms, we aim to streamline the teleoperation process, enabling operators to focus on high-level task objectives while the system autonomously manages low-level navigation and coordination tasks.

The rest of the paper is organized as follows. Sec. II introduces the teleoperation framework, whereas in Sec. III the devised control strategies are explained. The conducted experiments are described in Sec. IV, while Sec. V discusses their outcomes. Lastly, Sec. VI draws the conclusions of the paper, outlining possible further developments.

II. System Overview

The system reproduces the motion of a robotic swarm, controlled by a human operator via haptic interfaces through a narrow and tortuous path emulating a blood vessel or an industrial pipe.

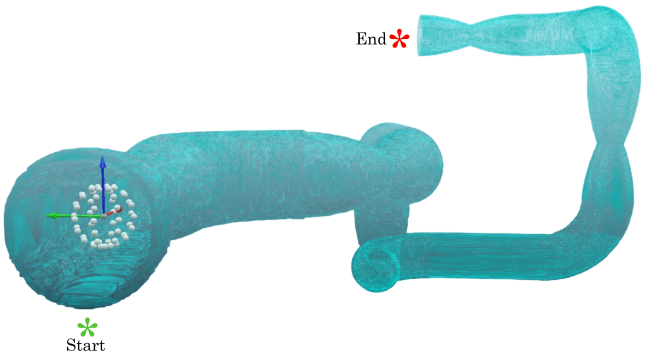

Fig. 2: Navigation path: the green and red stars indicate the beginning and end of the route, respectively.

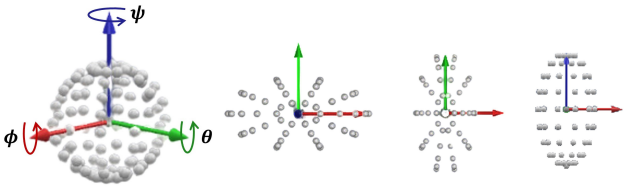

(a) (b)

Fig. 3: a) Swarm robot with its reference frame; the axes are represented in red (x), green (y), and blue (z). The angles ϕ, θ and ψ represent rotations referred to the swarm frame around its axes. b) Deformations of the swarm along the three axes of its reference system.

The virtual environment is developed in CoppeliaSim and graphically rendered using a desktop PC. The swarm is composed of 64 spherical agents initially arranged in a spherical formation with a depth sensor placed at its center. The target environment features straight and curved, deformed and non-deformed segments (turquoise-colored pipe in Fig. 2). As noticeable from the figure, we intentionally designed a complex pipe-like pathway to evaluate the operators' ability in adjusting the swarm's shape and trajectory during the navigation.

The pose and shape of the swarm can be controlled with 9 DoFs, being the pose of the swarm centroid 6 DoFs (i.e., position $\boldsymbol{p} = [x, y, z]$ and orientation $\boldsymbol{o} = [\phi, \theta, \psi]$) and 3 additional DoFs for modifying the shape along its three perpendicular axes of symmetry ($\boldsymbol{\delta} = [\delta_x, \delta_y, \delta_z]$). Fig. 3 visually reports the controllable degrees of freedom. The DoFs can be controlled either partially or entirely by one or two users utilizing a pair of Omega.7 haptic interfaces (Force Dimension, CH), depending on the specific conditions being considered. The Omega.7 interfaces enable users to collaboratively control the 9 DoFs of the robotic swarm. One haptic interface is for managing the pose of the swarm centroid (6 DoFs), while the other is dedicated to controlling the swarm deformation along its 3 axes of symmetry (3 DoFs). A generic deformation $\boldsymbol{\delta}$ along one of these axes results in an expansion or a contraction of the swarm by

moving its elements along that direction (see Fig. 3b). The deformation control ensures the swarm elements move along an ellipsoidal surface and prevents overlapping during expansion or contraction. Besides, deformation values are limited to avoid excessive contractions and stretching of the swarm. Deformation DoFs are essential for navigating complex environments, such as the one proposed in this work, which includes paths with varying geometries.

The mapping between the 9 DoFs of the swarm and the two interfaces is realized with an incremental strategy. The connection between the control interface and the controllable DoFs of the swarm is established by activating the clutch on the haptic devices. Consequently, when the clutch is activated, the poses of both the interface $\boldsymbol{h}(t_0)$ and the swarm $\boldsymbol{s}(t_0)$ are stored, allowing the operator to relocate the interface handle to a new position $\boldsymbol{h}(t_1)$. The difference $\Delta\boldsymbol{h}$ between $\boldsymbol{h}(t_0)$ and $\boldsymbol{h}(t_1)$ is calculated as follows:

$$\Delta\boldsymbol{h}^p = \boldsymbol{h}^p(t_1) - \boldsymbol{h}^p(t_0)$$
$$\Delta\boldsymbol{h}^o = \boldsymbol{h}^o(t_1)\boldsymbol{h}^o(t_0)^{-1},$$

where $\boldsymbol{h}^p \in \mathbb{R}^{3\times1}$ is the position vector and $\boldsymbol{h}^o \in \mathbb{R}^{3\times3}$ is the orientation matrix of the interface handle. Finally, $\Delta\boldsymbol{h}$ is transformed into the swarm reference system and added to $\boldsymbol{s}(t_0)$ to obtain the desired new pose. A similar approach can be applied to the deformation control. In addition to controlling the swarm, the system also provides users with both haptic and visual feedback crucial for improving performance in accomplishing the tasks. Indeed, in the event of a collision with the pipe wall, users receive vibrations on the handles of the haptic interfaces along with visual cues (i.e., the pipe-like path changes color from turquoise to red as in Fig. 1a).

ROS served as the framework between the two haptic interfaces, and CoppeliaSim was used to control the swarm robot and acquire data from the simulated environment.

III. Data-Driven Shared Control

This Section details the design of a shared-control strategy aiming at minimizing cognitive load while maximizing performance for a single teleoperator. Initially, we gathered and processed data from demonstrations involving two users simultaneously teleoperating the swarm using the two haptic interfaces. Leveraging data analysis techniques, we propose a framework for shared control of the swarm.

A. Data collection from dual-user experiments

The data collection procedure involved 10 subjects (5 males and 5 females, aged between 24 and 35 years, average age 28 $\pm$ 3.1). Among these participants, one had prior experience with teleoperation devices, providing a diverse sample in terms of familiarity with the technology used. The 10 participants were randomly paired into 5 groups. This randomization was aimed at minimizing biases related to individual skill level or prior experiences. Each pair formed a collaborative team for the duration of the data collection phase, jointly controlling the swarm across the designated pipe-like path (see Fig. 2). The experimental campaign followed the declaration of Helsinki, and there was no risk of harmful effects on subjects' health. Each participant gave written informed consent and was able to discontinue participation at any time during experiments. No payment was provided to the users. None of the participants reported any deficiencies in their visual or haptic perception abilities.

Users were introduced to the teleoperation system, asking them to: *i*) navigate through the pipe-like path as quickly as possible, *ii*) occupy with the robotic swarm the largest possible cross-sectional area within the path, and *iii*) minimize the number of collisions with the environment. Users were given a short period (2 minutes) to acquaint themselves with the system, followed by an initial practice session.

Each pair of users repeated the assigned task 6 times. In the first three trials, one user controlled the swarm pose while the second one managed its deformation. From the fourth to the last trial, the roles were reversed allowing each participant to experience both aspects of the swarm control (pose or deformation). In this scenario, the human operators fully controlled all the degrees of freedom of the swarm, without any autonomy involved.

The following metrics were used to evaluate the performance in accomplishing the requested task: *i*) the time necessary to complete the path t_p, *ii*) the percentage $A_c \in [0, 100]$ of path area occupied by the swarm along its section, and *iii*) the number of collisions n_c. Lower values of t_p and n_c indicate better performance, whereas A_c closer to 100 corresponds to a higher average occupied cross-sectional area. For our analysis, we treated the dual system as a single *Dual-Position-Orientation-Deformation* (D-POD) system, considering these metrics depended on both the users.

Additionally, subjective measures of cognitive load were collected through the NASA Task Load Index (NASA-TLX) questionnaire [18] for assessing the perceived workload across various dimensions, including Mental Demand, Physical Demand, Temporal Demand, Performance, Effort, and Frustration. This method evaluates the load using a 7-point scale, where each of the six questions is rated on a 21-level scale: 1 indicates "*very low*", while 21 indicates "*very high*".

Each participant was asked to complete the questionnaire twice, once after having controlled the pose (3 trials) and once after having controlled the deformation (3 trials) of the swarm. This approach insights into how each aspect of the control task contributed to the overall workload and how the allocation of responsibilities between pose and deformation control influenced the users' experience.

We collected a total of 30 data sets including both the users control inputs (i.e., positions $\boldsymbol{p}$, orientations $\boldsymbol{o}$ and deformations $\boldsymbol{\delta}$) and the depth data from the sensor.

B. Data analysis for variance estimation

In what follows, we present a systematic approach for analyzing the demonstration data using point cloud information.

The goal of this analysis is to determine which DoFs were most controlled during the trials. Initially, we developed a

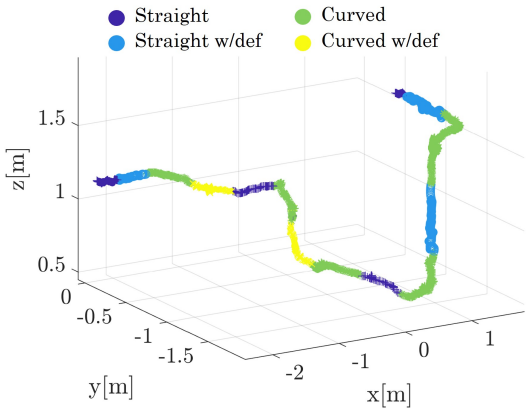

Fig. 4: A representative path labeled by the Gaussian Mixture Model clustering algorithm.

method to discretize the obtained data into shorter signals based on the similarities within the point clouds. This process started with the computation of Delaunay triangulation to partition the points into non-overlapping triangles. As second step, we constructed a dual Voronoi graph to determine the central path as its medial axis. Two parameters were then defined to quantify path curvature and deformation, achieved by comparing fitting errors from linear and quadratic splines along the central path.

Deformation values were assessed by evaluating the width of the cloud at various path locations. A Gaussian Mixture Model (GMM) clustering algorithm was thus applied to categorize the path into four types: straight non-deformed, straight deformed, curved non-deformed, and curved deformed. This classification process enabled the segmentation of demonstrations into labeled subsections for further analysis. Fig. 4 shows the application of this method in a representative trial. Note that this approach can be applied to paths of any shape, and consequently can be retrieved in real environment using standard imaging systems, e.g., 3D, CT scans.

After having classified the data into the different subsections, we proceeded to analyze how the users controlled the swarm DoFs, separately for each path type. Normalization and alignment of signals were performed to standardize measurements and compare operator performance, using Dynamic Time Warping (DTW) algorithm for temporal sequence alignment. We then evaluated inter-users variability among commanded positions, orientations, and deformations to identify trends in operator performance. To this aim, Pareto diagrams were utilized to analyze the datasets features' variance. Since we obtained similar results for all the different subsections, we ended the process with a unified analysis merging all subsets for a comprehensive evaluation of the data. As can be seen from Fig. 5, the analysis reveals that deformation exhibits the highest inter-users variability, while position demonstrates the least.

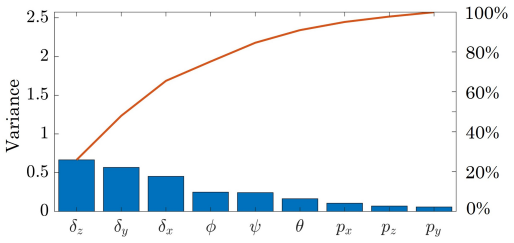

Fig. 5: Pareto diagram constructed by plotting the controlled DoFs along the x-axis, and their corresponding variances along the y-axis, in descending order. The right y-axis displays the percentage of the total variance.

C. Shared-control algorithms for multi-robot control

Human operators and autonomous algorithms collaborate on swarm control, with the sharing of authority depending on the task, environment, and user experience.

In applications in which the system is controlled by an expert operator in unstructured and/or dynamic environments (e.g., industrial maintenance, medical procedures), we expect users to prefer firsthand managing the DoFs that have been controlled with less arbitrariness during different demonstrations, i.e., those who have showed lower variabilities. Conversely, in applications in which the system is guided by a naïve operator in more structured environments (e.g., industrial or medical training), we expect the autonomous controller to take over the DoFs users controlled more similarly among the demonstrations.

As shown in Fig. 5, our analysis identified the greatest variability in the swarm deformations $\boldsymbol{\delta}$, meaning that these DoFs were controlled the most by users during the demonstrations. From this analysis, we proposed four shared control techniques, that share the available DoFs between one human user and the autonomous controller in different ways:

Single-Deformation (S-D): one user controls the swarm deformation (3 DoF, 65% of the total variance), the autonomous controller controls the swarm pose (6 DoF).

Single-Deformation-Orientation (S-DO): one user controls the swarm deformation and orientation (6 DoF, 90% of the total variance), the autonomous controller controls the swarm position (3 DoF).

Single-Position (S-P): one user controls the swarm position (3 DoF, 10% of the total variance), the autonomous controller controls the swarm orientation and deformation (6 DoF).

Single-Position-Orientation (S-PO): one user controls the swarm pose (6 DoF, 35% of the total variance), the autonomous controller controls the swarm deformation (3 DoF).

Table I summarizes the developed control technique reporting controlled DoFs and corresponding explained variance.

The controllers are based on vision data, where the information extracted from the point cloud as explained in Sec. III-B is exploited as reference for the controllers. In this way, our approach can generalize to new environments, eliminating the need for prior modeling.

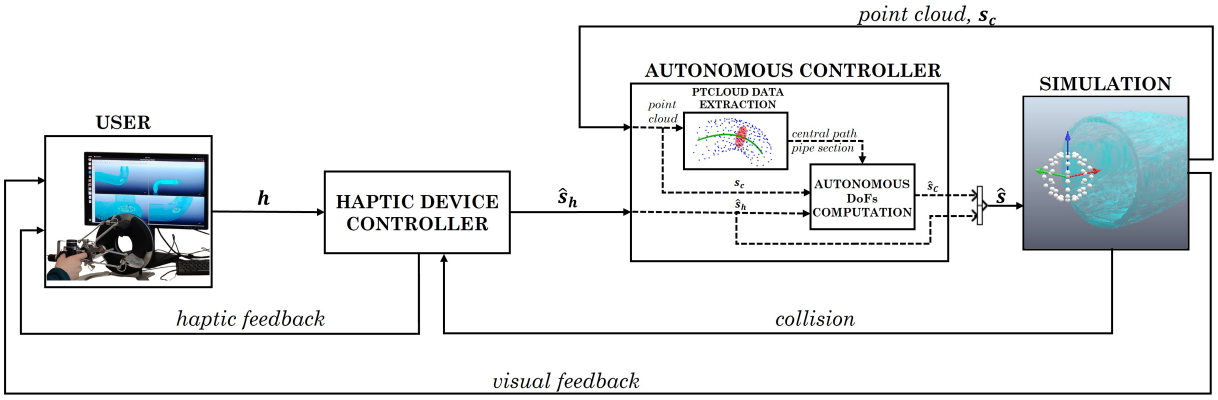

Fig. 6: Shared control scheme. The swarm state s includes position p, orientation o, and deformation δ. In each shared control strategy, the user is allocated control over a subset of the robot DoFs (s_h), while the other DoFs (s_c) are imparted by the autonomous controller. h indicates the pose of the haptic interface handle which is mapped into the desired state value $\hat{s_h}$. The autonomous controller outputs the desired robot state variables $\hat{s_c}$, based on the information about the pipe path extracted from the point cloud (central path and pipe section) and the current robot state. The final vector s is composed of $\hat{s_h}$ and $\hat{s_c}$

Control Technique	User Controlled DoFs	User Variance	Autonomous Controller Controlled DoFs	Autonomous Controller Variance
S-D	Deformation $(\delta_x, \delta_y, \delta_z)$	65%	Position (p_x, p_y, p_z) Orientation (ϕ, θ, ψ)	35%
S-DO	Deformation $(\delta_x, \delta_y, \delta_z)$ Orientation (ϕ, θ, ψ)	90%	Position (p_x, p_y, p_z)	10%
S-P	Position (p_x, p_y, p_z)	10%	Deformation $(\delta_x, \delta_y, \delta_z)$ Orientation (ϕ, θ, ψ)	90%
S-PO	Position (p_x, p_y, p_z) Orientation (ϕ, θ, ψ)	35%	Deformation $(\delta_x, \delta_y, \delta_z)$	65%

TABLE I: Developed control techniques. For each modality the controlled DoFs and the corresponding variance are reported, both for the user and for the autonomous controller.

The overall shared control scheme is shown in Fig. 6 where s_h refers to the DoFs controlled by the user through the haptic interfaces, while s_c refers to the DoFs governed by the autonomous controller.

When users are in charge of positions (S-P), the autonomous controller adjusts the swarm's shape to optimize the occupied area while avoiding collisions with the pipe's wall. Here, the autonomous control action s_c is represented by δ_c, which is computed as $\delta_c(t+1) = \delta_c(t) + u_\delta$, where the control input u_δ is proportional to the deformation error, defined as the difference between the ideal and the current deformation. The ideal deformation accounts for the swarm's distance from the central path, optimizing the occupied area while avoiding collisions with the pipe's wall.

In S-D, the autonomous controller regulates the positions to minimize the distance between the center of the swarm and the path while maintaining the elements of the swarm as close as possible to the borders of the tube. Here, the autonomous control action s_c is represented by p_c, which is defined as $p_c(t+1) = p_c(t) + u_p$, where u_p, similarly to S-P, is proportional to the position error, defined as the difference between the path center and the current swarm center. We did that to provide users with visual feedback and ensure consistency in pose and deformation control methodologies. In both control modes, the swarm is oriented in order to have its x axis pointing towards the direction of motion. The working principle of S-PO and S-DO is the same as the previous controllers, but differently the users are in charge of orientations.

In addition to these four shared control techniques, for the sake of comparison, we consider two standard human-in-the-loop teleoperation conditions, where the human operator retains complete control (no autonomy), i.e.,

Single-Position-Orientation-Deformation (S-POD): one user controls both the swarm pose (6 DoF) and deformation (3 DoF).

Dual-Position-Orientation-Deformation (D-POD): one user controls the swarm pose (6 DoF), another user controls the swarm deformation (3 DoF). This modality was used in Sec. III-A for the data collection).

The allocation of the control DoFs between the two Omega.7 interfaces is the same as in Sec. III-A.

IV. Experimental Evaluation

In this Section, we describe the experiments conducted to evaluate the shared-control strategies described in Sec. III-C. The same 10 subjects who participated in the initial data collection phase of Sec. III-A were involved in this experimental evaluation.

The experimental protocol was designed to conclude within a maximum duration of sixty minutes per participant, aiming to minimize fatigue and ensure a high engagement throughout the session. Participants received a briefing on the objectives and a 2-minute training session to familiarize themselves with the control techniques.

Each participant was asked to navigate the swarm through the pipe-like path described in Sec. II three times per control

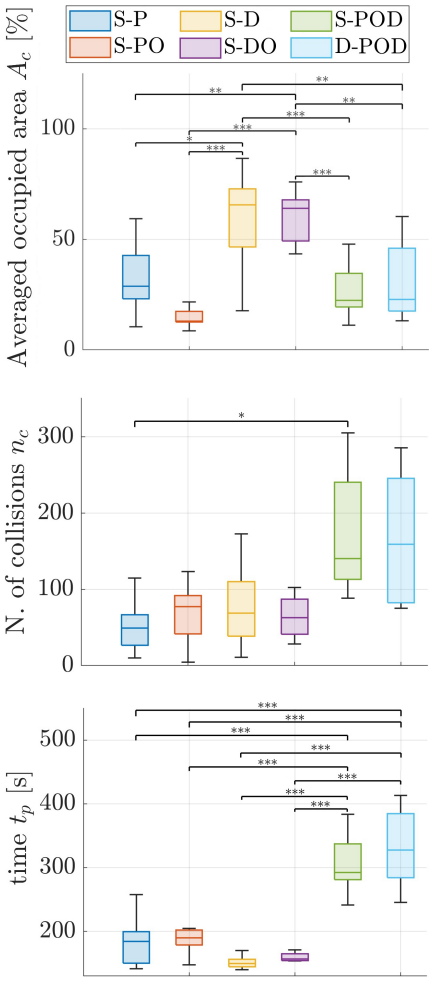

Fig. 7: Comparison of the quantitative metrics. Median and interquartile range of the six conditions are plotted. p-values are reported above the bar charts. The symbols $*$, $**$, and $***$ denote the levels of statistical significance.

condition, for a total of 15 trials (3 repetitions $\times$ 5 controls: S-D, S-DO, S-P, S-PO, S-POD). We did not carry out new repetitions in the D-POD control condition, as it had already been tested during the data collection phase (see Sec. III-A). As described in Sec. III-A, participants were asked to steer the swarm across the pipe-like path as fast as possible and occupy the largest possible cross-sectional area while minimizing the number of collisions with the environment. To mitigate potential learning biases, the presentation order of the control conditions to the users was randomized.

After each task, participants were asked to complete a NASA-TLX questionnaire to assess their subjective cognitive load. We also recorded quantitative performance metrics, i.e., the task completion time t_p, the average normalized cross-sectional area of the path occupied by the swarm A_c, and the number of collisions n_c, as in Sec. III-A.

V. Results and Discussion

This Section presents and discusses the outcomes of the experimental evaluation.

Data across the three repetitions from the same subject and control condition were averaged. Values that lay beyond 1.5 times the interquartile range (IQR) from the first (Q1) and third (Q3) quartiles were considered outliers, We identified and removed from the analysis three outliers within our dataset associated with the temporal metric t_c. Specifically, their values surpassed the aforementioned threshold, indicating significant deviation from the typical trial durations. Data were normally distributed as assessed by the Shapiro-Wilk test ($p > 0.05$). A one-way repeated-measures ANOVA was employed to analyze metrics t_c (time) and A_c (occupied area), whereas we carried out a Friedman test to analyze n_c (collisions), as this variable is measured on an ordinal scale. A post-hoc analysis employing a Bonferroni correction was conducted to identify differences between the conditions. This adjustment is crucial in multi-comparison scenarios to mitigate the risk of type I errors, i.e. to reduce possible false positive results.

The NASA-TLX questionnaire results were weighted to reflect the relative importance of each workload dimension. Subsequently, a Friedman non-parametric test was applied to these weighted scores to assess significant differences among the controllers we developed. This analysis was instrumental in confirming the distinctions in perceived workload and cognitive demands associated with each control strategy[1].

A. Quantitative metrics

Fig. 7 shows the results for the objective metrics. Overall, all the four shared control techniques (S-D, S-DO, S-P, S-PO) present statistically significant improvements compared to single- (S-POD) and dual-user (D-POD) standard teleoperation controls.

Results also suggests that each of the four shared control techniques offers distinct advantages. The control strategies in which the user directly controls the swarm deformation (S-D, S-DO) demonstrate high performance in maximizing the swarm's occupied area during navigation, indicative of an effective space utilization. S-D displays a median score of 65.63 with a Q1-Q3 range of 46.54-72.88, while S-DO records a median of 64.02 within a more compact range of 49.31-67.9. Furthermore, both modalities contribute to a notable reduction in terms of task completion time, signifying their operational efficiency. The consistency of these results is reflected in the interquartile ranges, indicating reliable performance across trials.

Control strategies with direct user control over swarm position (S-P, S-PO) yielded different results. The S-P control strategy not only presents good performance indicators in terms of occupied areas, but it also enhance users precision, resulting in significantly fewer collisions and lower task completion time with respect to the standard S-POD and D-POD control strategies. Conversely, S-PO is the control condition that led to the worst results. It showed the lowest median for the occupancy area A_c (Mdn: 13.15, Q1-Q3:12.72-17.52);

[1]For NASA-TLX analysis, the D-POD analysis was split in D-PO and D-D as users filled questionnaires for both pose and deformation.

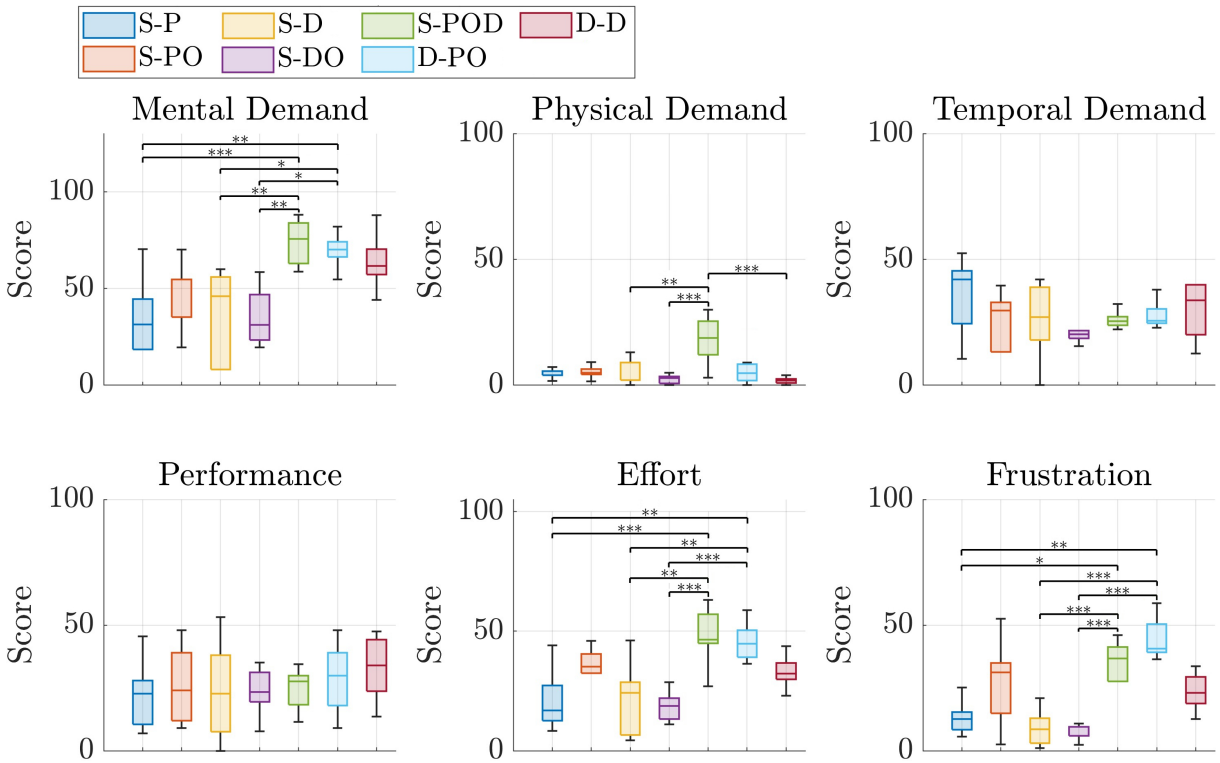

Fig. 8: Comparison of the NASA-TLX for all the tasks. Mean and standard deviation are reported for all the conditions. p-values are reported above the bar charts.

however, it still outperforms in terms of completion time the two standard teleoperation modalities S-POD and D-POD.

We can also appreciate how the shared control techniques show significantly lower variability with respect to S-POD and D-POD, reflecting inconsistent performance when participants had to control all the available DoFs. This inconsistency is likely due to the higher manual dexterity required, which led to both high variability in the results as well as generally worse performance. However, S-POD did not lead to significantly better performance than D-POD. Indeed, we expected that collaborating with another user would have led to worse performance, also considering that all subjects carried out the task in the D-POD condition first.

B. Qualitative metrics

Fig. 8 shows the results for the subjective metrics. The subjective findings align with the objective analysis discussed above. This quantitative evidence is mirrored in the subjective experiences of participants, as captured in the data from the NASA-TLX scores.

The weighted NASA-TLX results presented in the boxplot reflect differences in perceived workload among the various control strategies. It's notable that strategies involving deformation control (S-D and S-DO) show significantly lower scores in mental demand with respect to S-POD and D-PO. This reduction points to an improved user experience, suggesting that the deformation control strategies may align better with the operator's capabilities, leading to a more intuitive and less mentally taxing interaction. The congruence between these subjective assessments and the objective performance metrics underscores the effectiveness of these control strategies in both perceived and actual ease of use, enhancing overall satisfaction with the system's performance. Additionally, participants positively evaluate the S-P controller in terms of mental demanding (Mdn:31, Q1-Q3: 18.5-44). Overall, all the developed shared controllers are less cognitively demanding than full manual control modalities.

Regarding physical load, participant feedback generally indicates a low physical demand among the controllers. Notably, the S-POD modality exhibits considerable variability (Mdn: 18.75, Q1-Q3: 12-25.5), likely due to the complexity of manipulating dual interfaces simultaneously, thus increasing the physical engagement required. Furthermore, compared to the deformation controllers (S-D, S-DO, and D-D), bimanual control physical demand is significantly higher.

Temporal demand was perceived similarly across all control modalities, indicating no perceivable difference in the pressure to perform tasks quickly. Lower temporal demand values were noted for autonomous trajectory control of the swarm (S-D and S-DO). However, there are no significant differences, as the perception of individual users is very variable, as can be seen in the wide interquartile range of S-D, Q1-Q3:18-39. Conversely, position controls (S-P and S-PO) and manual controls (S-POD and D-PO) exhibited narrower interquartile ranges, indicating a more uniform user experience in terms of temporal pressure.

While the NASA-TLX scores for performance do not show statistically significant differences among the various

	S-P	S-PO	S-D	S-DO	S-POD	D-PO	D-D
Overall Weighted Workload Score	41.58	52.83	**38.2**	**35.6**	72.07	70.25	58.8

TABLE II: NASA-TLX workload.

control modes, the participants generally gave lower performance ratings to the shared control strategies over direct teleoperation. Note that, for this metric, the lower the score the better the perception of success. This suggests that the shared control interfaces may enhance the user's perceived effectiveness in operating the swarm.

In assessing perceived effort, our shared control architectures evidently ease the workload on users. Specifically, the position control (S-P) and the deformation controls (S-D and S-DO) are associated with significantly less effort as per user feedback, in stark contrast to the direct controls, such as S-POD and D-PO. This distinction underscores the ergonomic advantage of shared control systems in user-system interaction.

Eventually, S-P, S-D, and S-DO control modes show marked reduced user frustration compared to the bimanual control (S-POD) and dual-user teleoperation (D-PO). This is likely due to the complexity of managing the swarm's position and orientation, which is inherently more demanding and can lead to increased frustration, as reflected by the higher median score (Mdn: 31.25, Q1-Q3: 2.5-52.5) observed in the S-PO pose control mode.

Overall, the subjective analysis reveals that our shared-control strategies statistically significantly reduce cognitive load, indicating reduced mental demand, effort, and frustration for the users.

For the sake of completeness and clarity, we report the total workload in Table II. It is evident that the deformation control strategies (S-D and S-DO) exhibited the lowest overall workloads, indicating an optimized user experience. These outcomes suggest a correlation between the measured performance improvements and the operators' perceived ease of use and satisfaction with the system.

VI. Conclusion and Future Works

In this work, we designed, implemented, and tested data-driven shared control strategies aimed at reducing the human cognitive burden on operators during the teleoperation of robot swarms while enhancing task performance. The proposed approach leveraged an initial data collection phase involving a dual-user teleoperation task in a 3D simulated complex environment. Analyzing the variability of the degrees of freedom controlled by the users, we designed four shared control policies which differ in the level of autonomy. The resulting controllers demonstrated the capacity to assist a single operator in managing a complex system with multiple degrees of freedom.

An extensive and careful evaluation, supported by a user study, confirmed that the developed controllers significantly reduce the cognitive load and improve the task performance. In particular, the best control modality turned out to be to automate the DoFs with less variability while leaving the user in control of the others; in this way, it is possible to create shared control strategies where the user can focus on the more subjective aspects of the task, i.e. the ones with more variability.

Future work will employ machine learning algorithms (e.g., Reinforcement Learning) to improve the presented controllers starting from the data gathered in this study. We will also explore the application of these strategies in more varied and dynamic environments to further validate their robustness and applicability in real-world scenarios (e.g., microrobot swarm navigation in blood vessels or drone navigation in constrained scenarios at the macroscale).

References

[1] J. Cortés and M. Egerstedt, "Coordinated control of multi-robot systems: A survey," *SICE Journal of Control, Measurement, and System Integration*, vol. 10, no. 6, pp. 495–503, 2017.

[2] R. N. Darmanin and M. K. Bugeja, "A review on multi-robot systems categorised by application domain," in *Proc. Mediterranean conference on control and automation (MED)*, 2017, pp. 701–706.

[3] Z. Lin, T. Jiang, and J. Shang, "The emerging technology of biohybrid micro-robots: a review," *Bio-Design and Manufacturing*, pp. 1–26, 2022.

[4] B. J. Nelson, S. Gervasoni, P. W. Chiu, L. Zhang, and A. Zemmar, "Magnetically actuated medical robots: An in vivo perspective," *Proceedings of the IEEE*, vol. 110, no. 7, pp. 1028–1037, 2022.

[5] B. Wang, K. Kostarelos, B. J. Nelson, and L. Zhang, "Trends in micro-/nanorobotics: materials development, actuation, localization, and system integration for biomedical applications," *Advanced Materials*, vol. 33, no. 4, p. 2002047, 2021.

[6] M. Luo, Y. Feng, T. Wang, and J. Guan, "Micro-/nanorobots at work in active drug delivery," *Advanced Functional Materials*, vol. 28, no. 25, p. 1706100, 2018.

[7] P. A. York, R. Peña, D. Kent, and R. J. Wood, "Microrobotic laser steering for minimally invasive surgery," *Science Robotics*, vol. 6, no. 50, p. eabd5476, 2021.

[8] X. Yan, Q. Zhou, M. Vincent, Y. Deng, J. Yu, J. Xu, T. Xu, T. Tang, L. Bian, Y.-X. J. Wang *et al.*, "Multifunctional biohybrid magnetite microrobots for imaging-guided therapy," *Science robotics*, vol. 2, no. 12, p. eaaq1155, 2017.

[9] J. Pan, J. Eden, D. Oetomo, and W. Johal, "Exploring the effects of shared autonomy on cognitive load and trust in human-robot interaction," *arXiv preprint arXiv:2402.02758*, 2024.

[10] D. A. Abbink, M. Mulder, and E. R. Boer, "Haptic shared control: smoothly shifting control authority?" *Cognition, Technology & Work*, vol. 14, pp. 19–28, 2012.

[11] M. Chiou, N. Hawes, and R. Stolkin, "Mixed-initiative variable autonomy for remotely operated mobile robots," *ACM Transactions on Human-Robot Interaction (THRI)*, vol. 10, no. 4, pp. 1–34, 2021.

[12] L. Iocchi, D. Nardi, M. Piaggio, and A. Sgorbissa, "Distributed coordination in heterogeneous multi-robot systems," *Autonomous robots*, vol. 15, pp. 155–168, 2003.

[13] M. Aggravi, G. Sirignano, P. R. Giordano, and C. Pacchierotti, "Decentralized control of a heterogeneous human–robot team for exploration and patrolling," *IEEE Transactions on Automation Science and Engineering*, vol. 19, no. 4, pp. 3109–3125, 2021.

[14] C. Jiang, Z. Chen, and Y. Guo, "Multi-robot formation control: a comparison between model-based and learning-based methods," *Journal of Control and Decision*, vol. 7, no. 1, pp. 90–108, 2020.

[15] A. Marino, C. Pacchierotti, and P. R. Giordano, "On the stability of gated graph neural networks," *arXiv preprint arXiv:2305.19235*, 2023.

[16] S. Baltrusch, F. Krause, A. de Vries, W. van Dijk, and M. de Looze, "What about the human in human robot collaboration? a literature review on hrc's effects on aspects of job quality," *Ergonomics*, vol. 65, no. 5, pp. 719–740, 2022.

[17] J. L. Plass, R. Moreno, and R. Brünken, "Cognitive load theory," 2010.

[18] S. G. Hart, "Nasa-task load index (nasa-tlx); 20 years later," in *Proceedings of the human factors and ergonomics society annual meeting*, vol. 50, no. 9. Sage publications Sage CA: Los Angeles, CA, 2006, pp. 904–908.